

## CFD Analysis of Sloshing in the Fuel Tank of a Heavy Vehicle with Emergency Braking System

Turan Alp Arslan<sup>1\*</sup>, Hüseyin Bayrakçeken<sup>1</sup> and Hicri Yavuz<sup>2</sup>

0000-0003-3259-4854, 0000-0002-1572-4859, 0000-0001-8427-5164

<sup>1</sup> Department of Automotive Engineering, Faculty of Technology, Afyon Kocatepe University, Afyon, 03200, Turkey.

<sup>2</sup> Department of Engine Vehicles and Transportation Technology, Vocational School of Afyon, Afyon Kocatepe University, Afyon, 03200, Turkey.

### Abstract

Liquid sloshing, which occurs in all accelerating and liquid-carrying vehicles, is of great importance, especially in the automotive and aerospace industries. Large-scale fluid sloshing causes both operational and safety problems in vehicles. In this study, the fuel tank of a heavy vehicle with an emergency braking system is designed in three dimensions, and liquid sloshing in the fuel tank is investigated by CFD analysis method. VOF solution method, k- $\epsilon$  turbulence model, and PISO solution algorithm are used in the study. In the analysis of liquid sloshing, it is assumed that the vehicle is traveling at a certain speed, decelerates and stops with emergency braking, and remains stationary for a while. The braking scenario and boundary conditions are based on test data from a heavy vehicle manufacturer. The designed fuel tank with a capacity of 207.6 liters was analyzed at 25%, 50%, and 60% diesel fuel filling levels in 6 different cases with and without anti-slosh baffles. Four virtual sensors were placed on the side wall of the fuel tank in the direction of vehicle movement, and time-dependent pressure changes were analyzed for all cases. In addition, the fuel volume ratio in all cases is visualized and presented for specific time steps. With the use of anti-slosh baffles, the maximum pressure, the rate of pressure increase, and the liquid sloshing were reduced by a factor of 2-3 for different cases. With the design of the fuel tank using anti-slosh baffles, instantaneous interruptions in the fuel system are prevented. Reducing the impact pressures on the tank walls is expected to positively affect noise, vibration, and stability problems.

Keywords: CFD; Emergency braking system; Fuel tank; Sloshing; Tank baffles; VOF

### Research Article

<https://doi.org/10.30939/ijastech..1360466>

Received 14.09.2023

Revised 27.10.2023

Accepted 12.11.2023

\* Corresponding author

Turan Alp Arslan

[talparslan@aku.edu.tr](mailto:talparslan@aku.edu.tr)

Address: Automotive Engineering Department, Faculty of Technology, Afyon Kocatepe University, Afyon, Turkey  
Tel:+902722182556

### 1. Introduction

The free surface motion or vibration of a fluid in a partially filled container stimulated by external forces is called sloshing [1-3]. Sloshing is defined as a complex phenomenon involving nonlinear properties of the fluid [4]. The free surface motion of the liquid in the tank depends on the shape and magnitude of the external forces, tank geometry, filling level, damping effect of the internal structure, and liquid properties [5]. These motions show different characteristics such as planar, non-planar, symmetric, asymmetric, turbulent, random shock, quasi-periodic and chaotic [6-8]. Liquid sloshing occurs especially intensively in automotive fuel tanks, liquid transportation containers, sea, air, and space vehicles, petrochemical storage, seismically stimulated storage areas, dams, and nuclear power plants and causes both operational and safety problems in all these areas [9,10].

Sloshing occurs in all vehicles that move with acceleration and carry liquids. The study of this complex fluid-structure interaction is of great importance, especially in the automotive and aerospace fields [11]. In addition to space, air, and sea vehicles, partially filled tanks of land vehicles such as cars, trucks, and buses are subjected to severe sloshing due to acceleration. Liquid sloshing, which causes high impact pressures on the tank walls, can cause structural damage and destabilization of the vehicle carrying the tank [12]. With inappropriate fuel tank designs, large-scale sloshing occurs, causing sudden interruptions in the fuel system and increasing fuel vapor, which leads to hydrocarbon (HC) emissions in gasoline vehicles. In addition, the amount of noise and vibration transmitted to the passenger compartment increases with the sloshing that occurs during sudden acceleration, sudden deceleration,

cornering, and driving on rough roads [13]. Various design solutions are put forward to prevent all these problems. The most common of these is the addition of different geometry and number of anti-slosh baffles in the tank [14]. However, using anti-slosh baffles, which minimize the free surface movement and the adverse effects caused by dividing the fuel tank into smaller volumes, increases the tank weight and production costs.

Thanks to the advantages it offers, the finite element method is frequently used in the design of vehicle and machine parts [15-18]. Nowadays, both anti-slosh and weight and cost reduction studies in fuel tank design are carried out by computational fluid dynamics (CFD) method using special software [19,20]. With the CFD method, all properties and parameters such as acceleration, force, flow regime, liquid properties, tank geometry, filling level, anti-slosh baffle geometry, number, and location can be tested in different combinations to determine the optimum design. Unlike experimental studies, these analyses are reproducible, cost-effective, and time-saving [21-23]. Various numerical methods are used for the sloshing analysis of fuel tanks by the CFD method. The common ones are explicit finite element, arbitrary Lagrangian-Eulerian (ALE), hybrid finite element, smoothed particle hydrodynamics (SPH), and volume of fluid (VOF) [24,25]. Developed by Hirt and Nichols [26] to study the complex free surface motion of incompressible fluids, VOF is a robust and flexible method compared to other numerical methods [27]. It is seen that CFD analysis management and the VOF solution method are widely used in the literature for the simulation of the sloshing of two or more types of immiscible fluids in a tank [28-33].

Liquid sloshing can occur in the form of laminar or turbulent flow. Numerical methods for solving turbulence problems are based on potential flow theory or Navier Stokes equations [34]. No clear consensus exists on whether turbulence models should be used for fluid turbulence [35]. Potential flow theory and some analytical methods can be used for laminar flow owing to their relatively stable solutions and low computational effort [36]. However, while acceptable results are obtained from simulation studies without turbulence models, it has been proved that using turbulence models improves solution accuracy and efficiency [37]. Therefore, the inclusion of an appropriate turbulence model in the liquid sloshing problem is important for simulation success. The standard k-ε turbulence model, the RNG k-ε turbulence model, the realizable k-ε turbulence model, and the k-ω SST turbulence model are the turbulence models commonly used in the analysis of fluid turbulence [38]. The standard k-ε turbulence model stands out with its high prediction accuracy and fast convergence in studies of impact pressure. The use of the k-ω SST turbulence model is recommended for studies of free surface motion owing to its high accuracy [39].

In this study, the sloshing phenomenon in the fuel tank of a heavy vehicle with an emergency braking system (EBS) is investigated by CFD analysis. VOF solution method and k-ε turbulence model are used in the study. In order to monitor the fluid sloshing, it is assumed that the vehicle is traveling at a certain speed, decelerates and stops with emergency braking, and remains stationary for a while. The designed fuel tank with a capacity of 207.6 liters

was analyzed at 25%, 50%, and 60% diesel fuel filling levels, with and without anti-slosh baffles, in 6 different cases. Time-dependent pressure changes were obtained for all cases with 4 virtual sensors positioned on the side wall of the tank in the direction of vehicle movement. In addition, the fuel volume ratio in all cases was visualized and analyzed for specific time steps. In the study, it is aimed to minimize the impact pressures, noise, and vibration on the tank walls and to prevent instantaneous interruptions in the fuel system by minimizing the sloshing phenomenon with the use of anti-slosh baffles.

## 2. Materials and Methods

The CFD analysis of the sloshing phenomenon in a heavy vehicle fuel tank with an EBS system has been carried out in Ansys Fluent software. The simulation study was completed in four stages. In the first stage, the fuel tanks of the heavy vehicle were designed in three dimensions, and filling levels and fuel properties were determined. In the second stage, the mesh structures of the tank models were created, and the adequacy of these structures was verified with the literature. In the third stage, the braking scenario and boundary conditions are defined using the test data taken as reference. In the last stage, analysis methods and solution algorithms suitable for the specified purpose are applied, and the results are evaluated.

### 2.1 Governing Equations

A mathematical model is created using partial differential equations, integral equations, and boundary conditions in CFD applications. The performed sloshing analysis provides solutions using the volume fraction equation, the momentum equation, and the standard k-ε turbulence model. The volume fraction equation, also called the continuity transport equation, is given by Eq. (1).

$$\frac{1}{\rho_i} \left[ \frac{\partial}{\partial t} (\alpha_i \rho_i) + \nabla (\alpha_i \rho_i \vec{v}_i) \right] = S_{\alpha_i} + \sum_{p=1}^n (\dot{m}_{pi} - \dot{m}_{ip}) \quad (1)$$

Where  $\alpha$ ,  $\rho$ , and  $\vec{v}$  represent the volume fraction, density, and velocity for phase i, respectively.  $\dot{m}_{xy}$  is the mass transfer from phase x to phase y. The momentum equation is shown in Eq. (2).

$$\rho \left( \frac{\partial v}{\partial t} + v(\nabla v) \right) = -\nabla P + \nabla \tau + \rho g \quad (2)$$

In this equation,  $t$  is time,  $\nabla$  is divergence,  $P$  is pressure,  $\tau$  is stress, and  $g$  is gravitational acceleration. Finally, the turbulence kinetic energy ( $k$ ) and its dissipation rate ( $\epsilon$ ), which form the k-ε turbulence model, are given by Eq. (3) and Eq. (4), respectively.

$$\frac{\partial}{\partial t} (\rho k) + \frac{\partial}{\partial x_i} (\rho k u_i) = \frac{\partial}{\partial x_i} \left[ \left( \mu + \frac{\mu_t}{\sigma_k} \right) \frac{\partial k}{\partial x_j} \right] \dots \dots + G_k + G_b - \rho \epsilon - Y_M + S_k \quad (3)$$

$$\frac{\partial}{\partial t} (\rho \epsilon) + \frac{\partial}{\partial x_i} (\rho \epsilon u_i) = \frac{\partial}{\partial x_i} \left[ \left( \mu + \frac{\mu_t}{\sigma_\epsilon} \right) \frac{\partial \epsilon}{\partial x_j} \right] \dots \dots + G_{1\epsilon} \frac{\epsilon}{k} (G_k + C_{3\epsilon} G_b) - G_{2\epsilon} \rho \frac{\epsilon^2}{k} + S_\epsilon \quad (4)$$

Where  $\mu$  is the viscosity,  $\mu_t$  is the turbulent viscosity,  $\sigma_x$  is the turbulence Prandtl number for  $x$ ,  $G_k$  is the turbulent kinetic energy due to mean velocity gradients,  $G_b$  is the turbulent kinetic energy due to buoyancy,  $Y_M$  is the contribution of the fluctuating dilatation in compressible turbulence to the overall dissipation rate,  $S_x$  is the user-defined source for  $x$ ,  $G_{1\varepsilon}$ ,  $G_{2\varepsilon}$ , and  $C_{3\varepsilon}$  are the model constants.

**2.2 Fuel Tank Model and Fuel Properties**

In the first stage of the study, the fuel tank planned for use in a heavy vehicle, is designed in two different types, with and without baffles. Solidworks software was used in the three-dimensional design phase. The designed fuel tanks are shaped like a rectangular prism, common in today's heavy vehicles, and have a fuel capacity of 207.6 liters. It is seen that this capacity is sufficient for a pickup truck or midi bus. The tanks are equipped with a filling cap, fuel transfer pipe, float system, drain valve, and connection brackets. The designed fuel tanks are 1200 mm long, 350 mm high, and 510 mm wide. Inside the tank, there are two anti-slosh baffles with a height of 250 mm and a thickness of 3 mm. These baffles, which provide fuel flow between the volumes with the help of holes at the bottom, are placed symmetrically in the tank at equal distances from the side walls. Some geometric simplifications were made on both types of fuel tank models in order to shorten the solution time and improve the quality of the mesh structure.

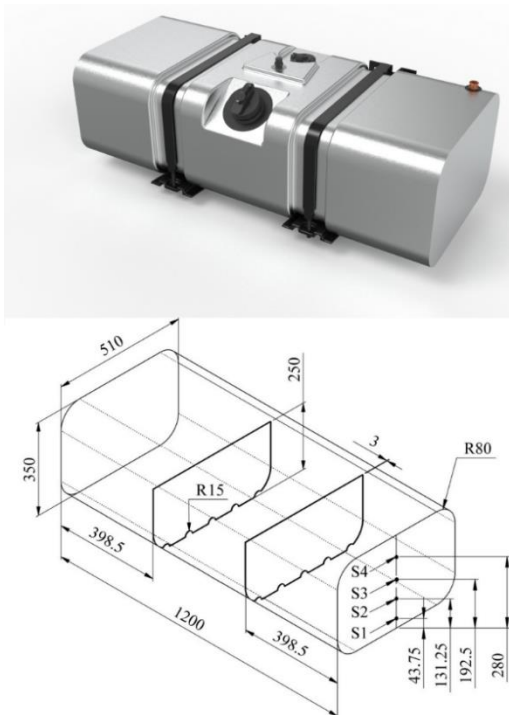


Fig. 1. Fuel tank model dimensions and virtual sensor locations

Four virtual sensors coded S1, S2, S3, and S4 were positioned on the side wall of the tanks in the direction of vehicle motion to investigate the time-dependent pressure variations. The designed fuel tank model, basic dimensions, and sensor locations are shown in Figure 1. Analyses were carried out on the fuel tanks at 25%,

50%, and 60% filling levels, with and without anti-slosh baffles, in 6 different cases. In these analyses, diesel fuel with a cetane number of 45, selected from the Ansys library, was preferred. Detailed specifications of the diesel fuel used are presented in Table 1.

Table 1. Fuel properties.

Fuel Properties (Units)	Values
Fuel type	Diesel
Cetane number	45
Density (kg/m <sup>3</sup> )	846
Viscosity (kg/m-s)	0.0029
Molecular weight (kg/kmol)	180.33

**2.3 Meshing Strategy and Analysis Methods**

Mesh structure creation on the fuel tank models was performed with the Ansys software Mesh module. In order to minimize the deviations in the results in both fuel tank models, a mesh structure with equal properties was used. In this study, where liquid surface motion is mainly investigated, tetrahedral elements with 10 nodal points, which provide highly accurate solutions in surface contours, are preferred. Although the solution time increases slightly with the use of tetrahedral elements with a large number of nodes, the quality, and accuracy of the results obtained improve [40]. Geometric changes that occur in the analysis of systems with dynamic structure cause the quality of the mesh structure to decrease over time, leading to a decrease in solution accuracy. In order to prevent these degradations and to keep the mesh quality at a high level during the whole analysis process, the adaptive mesh method is used. The adaptive mesh structure performs 7 resolutions to rebuild the mesh structure from coarse to fine. Table 2 shows the number of elements and nodes of the mesh structures used in all filling levels of the fuel tank models. In the fuel tank model with anti-slosh baffles, the number of elements and nodes increased due to the relatively small hole details at the bottom of the sheet metal baffles.

Table 2. Mesh details.

Fuel Tank Models	Element Type	Number of Elements	Number of Nodes
Without baffle	Tetrahedral	65876	339618
With baffle		91586	483032

The quality of the mesh structure is directly related to the distribution and uniformity of the elements. Significant dimensional differences and shape changes between adjacent elements impair solution stability [41]. After creating the mesh structure of the fuel tank models, the quality parameters of the mesh structure were checked, and the validity of this structure was verified with the literature data. Mesh structure quality parameters, current values, recommended limits, and adequacy of the mesh structure are presented in Table 3. In the study where three different quality parameters, namely aspect ratio, orthogonality, and skewness, were considered, it was determined that the mesh structures created for both tank models were suitable and acceptable for the analysis solution.

Table 3. Mesh quality parameters.

Models	Parameters	Values	Recommended	Adequacy
Without baffle	Max. aspect ratio	10.431	<40	Good
	Min. orthogonality	0.172	>0.15	Acceptable
	Max. skewness	0.827	<0.95	Acceptable
With baffle	Max. aspect ratio	15.02	<40	Good
	Min. orthogonality	0.153	>0.15	Acceptable
	Max. skewness	0.846	<0.95	Acceptable

**2.4 Bounding Conditions and Analysis Setup**

The heavy vehicle in which the fuel tank sloshing event is analyzed is traveling at 80 km/h, braking suddenly with EBS and stopping at 40 m. In order to simulate the braking scenario and the sloshing event as closely as possible, the speed and stopping distance values are taken from the test data of a heavy vehicle manufacturer. Eq. (5) calculates stopping distance using vehicle speed and stopping time, while Eq. (6) calculates stopping distance using vehicle speed and braking acceleration [42].

$$S = V_0 t_r + \frac{V_0 t_s}{2} \tag{5}$$

$$S = V_0 t_r + \frac{V_0^2}{2a_b} \tag{6}$$

Where  $S$  is stopping distance,  $V_0$  is vehicle speed,  $t_r$  is reaction time,  $a_b$  is braking acceleration, and  $t_s$  is stopping time.

Table 4. Bounding conditions.

Bounding Conditions (Units)	Values
Assist braking system	EBS
Initial velocity (km/h)	80
Stopping distance (m)	40
Braking acceleration (m/s <sup>2</sup> )	6.1716
Braking duration (s)	3.6

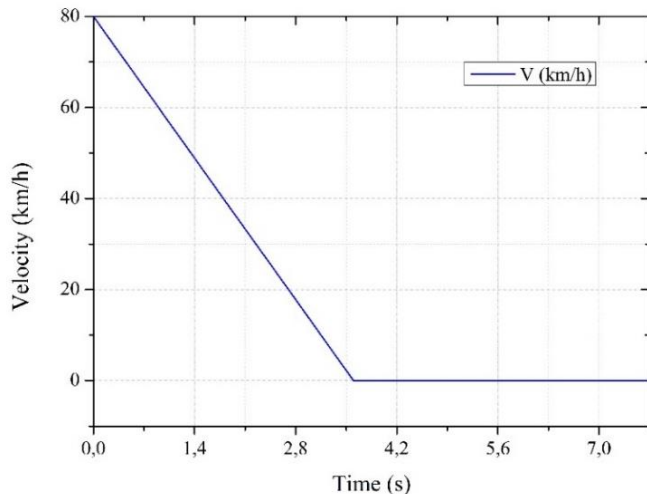


Fig. 2. Velocity vs time graph of the vehicle

The reaction time is neglected since the analysis starts with braking, and acceleration will act on the tank from the start of braking. As in the reference test, the vehicle is assumed to brake and stop with minimum slip and maximum efficiency on dry asphalt. The braking scenario and boundary conditions are presented in Table 4. The horizontal braking acceleration of 6.1716 m/s<sup>2</sup> and vertical gravity acceleration of 9.81 m/s<sup>2</sup> obtained from the equations are applied on the fuel tank. In the analyses performed, the vehicle brakes for 3.6 seconds and stops and remains stationary for 4.1 seconds for the damping of the sloshing phenomenon. The velocity-time graph of the heavy vehicle is shown in Figure 2.

Fuel tank sloshing analyses were performed in the transient regime in Ansys Fluent software. In the analysis setup, the VOF method and the k-ε turbulence model were used to analyze the fluid surface motions, which provide stable and highly accurate results compared to other methods. Although there are many different approaches to modeling flow motions in CFD analysis studies, the k-ε turbulence model stands out in solving engineering problems with its practical use and high-accuracy results [43,44]. The PISO algorithm, which is recommended for analysis in the transient regime and where mesh structure distortions are intensively observed, is chosen as a solution method. With this algorithm, stable solutions are obtained in large time steps, and the computational effort is reduced [45]. In the study, each sloshing analysis was generated with 110 time steps with a magnitude of 0.07 seconds, covering a total period of 7.7 seconds. The fuel tank sloshing analysis methods are presented in detail in Table 5.

Table 5. Sloshing analysis methods.

Analysis Methods (Units)	Values
Solver type	Pressure-Based
Time	Transient
Model	Multiphase, VOF
Viscosity	k-ε (standart)
Solution method	PISO
Materials	Air and Diesel
Analysis duration (s)	7.7
Time step size (s)	0.07
Number of time steps	110
Maximum iterations / Time step	20

**3. Results and Discussion**

As a result of the sloshing analyses, time-dependent pressure values were recorded from virtual sensors placed on the side wall of the fuel tank in the direction of vehicle movement for all cases. Figure 3 shows the pressure changes in the tank designs with and without anti-slosh baffles for 25% diesel fuel filling level. From the start of the heavy vehicle braking with EBS, the pressure on the fuel tank wall without baffles increased sharply. At 0.525 seconds, the pressure on the sensors reached its maximum value. At this moment, the maximum pressure measured at the sensor coded S1 was 4252.92 Pascal. Afterward, the pressure decreased slightly depending on the braking acceleration and the amount of sloshing and fluctuated and remained at high values until the end of braking

at 3.6 seconds. As the braking ended and the vehicle came to a standstill, the diesel fuel moved towards the opposite wall of the tank, causing a sudden decrease in the pressure. However, in this tank, where there were no anti-slosh baffles, the pressure measured from the sensors continued fluctuating at high values throughout the analysis due to the large-scale sloshing effect. In the fuel tank where anti-slosh baffles were used, there was a significant improvement in the rate of pressure rise and maximum pressure. In this tank, the initial peak pressure measured from the sensor coded S1 was 1508 Pascal at 0.7 seconds. Until the end of the braking event, the pressure in this tank increased gradually due to the fuel passage between the volumes. However, it is clear from the graphs that this increase is balanced, and the sloshing is minimized. At the end of braking at 3.6 seconds, the pressure on the wall where the sensors were positioned decreased sharply with the reverse movement of the fuel. Then, until the end of the analysis, small sloshing events were damped, and the fuel in the tank stabilized.

design with and without anti-slosh baffles. In the tank model without the anti-slosh baffle, a sudden accumulation of fuel on the tank wall and a rapid pressure increase occurred upon braking. At 0.42 seconds, the pressure values reached a maximum and were measured as 6120.43 Pascal on the sensor coded S1. Then, with continued braking, the pressure decreased slightly and remained at high values until 3.6 seconds in a partially fluctuating manner. With the end of braking, a rapid pressure drop followed by a high amount of sloshing was observed. At this filling level, severe sloshing persisted even at the end of the analysis at 7.7 seconds. In the fuel tank where the anti-slosh baffle was used, there was no sudden increase in pressure with increasing filling level as in the 25% filled tank. A reasonably balanced pressure increase and fuel passage between the volumes occurred at this design and fill level. Until approximately 3.22 seconds at the end of braking, the fuel smoothly transitioned to the volume in the direction of travel and gradually increased the pressure. At this moment, the maximum pressure was measured as 3000.43 Pascal via the sensor coded S1. With the end of the braking, the fuel moving to the opposite volumes in the tank decreases the pressure on the sensors. Again, it is seen that the sloshing is minimized until the end of the analysis with the steady flow of fuel over time.

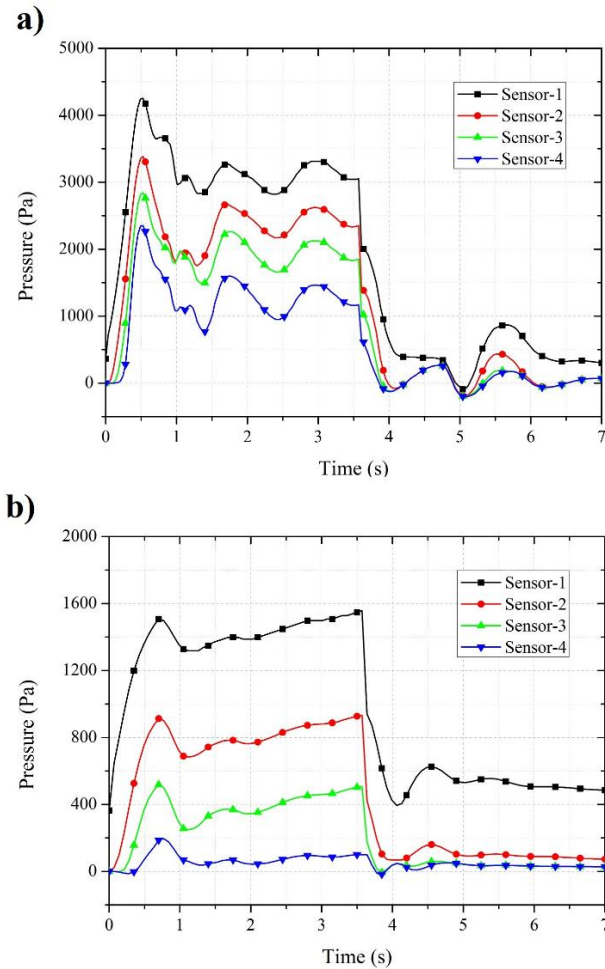


Fig. 3. The pressure history curves of sloshing for a) 25% fill level without baffle and b) 25% fill level with baffle

Figure 4 shows the pressure changes in the tank designs with and without anti-slosh baffles for 50% diesel fuel filling level. When the graphs are analyzed, it is seen that with increasing filling level, the liquid movement in the tank is more stable for both the

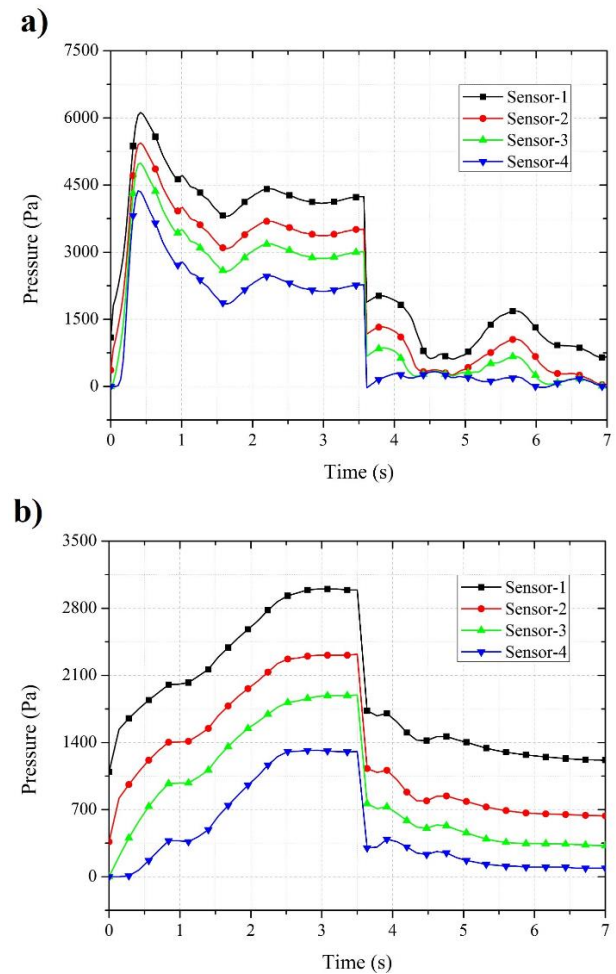


Fig. 4. The pressure history curves of sloshing for a) 50% fill level without baffle and b) 50% fill level with baffle

Figure 5 shows the pressure changes in the tank designs with and without anti-slosh baffles for 60% diesel fuel filling level. In the tank design without anti-slosh baffles, a sudden fuel pressure hits the tank wall, and the pressure partially fluctuates until 3.6 seconds and remains at high values. Here, the maximum pressure was measured as 6229.75 Pascal at 0.35 seconds via the sensor coded S1. With the increase in the filling level, the sloshing decreased slightly, and the stability of the fluid movements increased. After braking, when the vehicle became stationary, a high rate of sloshing occurred, and the fluid stability decreased. In the fuel tank design with anti-slosh baffles, there are improvements in the pressure increase and the rate of pressure increase. The maximum pressure reached 3729.75 Pascal in 2.1 seconds on the sensor coded S1 and remained approximately at this value until the end of braking. After braking, minimal fluid movements and sloshing with minimal irregularity were observed. Until the end of the analysis, the pressure gradually decreased slightly with regular fuel flow between the volumes. It was determined that the pressure changes measured over the sensors coded S1, S2, S3, and S4 were in similar forms and that the amount of pressure increased only with the increase in height due to the sensor positions. It is seen that the use of anti-slosh baffles has significant effects on impact pressure and liquid sloshing in all 25%, 50%, and 60% diesel fuel filling levels. The maximum pressure, rate of pressure increase, and liquid sloshing decreased by about 2-3 times for different cases using anti-slosh baffles. It is thought that this will prevent damage to the tank walls, noise, vibration, instability on the vehicle carrying the tank, fuel system interruptions, and increase in HC emissions in gasoline vehicles.

The fuel volume fraction results for all diesel fuel fill levels and fuel tank designs are shown in Figure 6, where the liquid sloshing is visualized and presented. The results cover the entire analysis period of 7.7 seconds with 0.7 second time step intervals. The fluid movements seen in the figure support the pressure changes measured by the virtual sensors. In tank designs without anti-slosh baffles, the braking acceleration acting with the start of the analysis causes large-scale liquid sloshing on the fuel. Although the amount of sloshing decreases with the increase in the filling level, the fuel is completely withdrawn from the tank center as all the fuel accumulates on the side wall. With this situation, interruptions in the fuel system become inevitable. With the end of braking, the fuel suddenly hits the opposite wall again. Fuel movement with sudden acceleration changes at the beginning and end of braking can cause damage, noise, and vibration on the tank walls. Liquid sloshing is minimized in tank designs where anti-slosh baffles are used. The division of the fuel tank into three separate volumes with baffles reduces the sudden pressure increase and maximum pressure on the side walls. Fuel passage through the holes at the bottom of the baffles is smooth and gradual. This situation ensures that there is always some fuel in the tank bottom and prevents interruptions in the system. In addition, the decrease in pressure rise is expected to prevent damage to the tank walls, noise, and vibration. Considering the fuel flow, pressure values, amount of sloshing, production costs and fuel tank weight, the partitioned tank design is considered sufficient for a heavy vehicle moving with low accelerations.

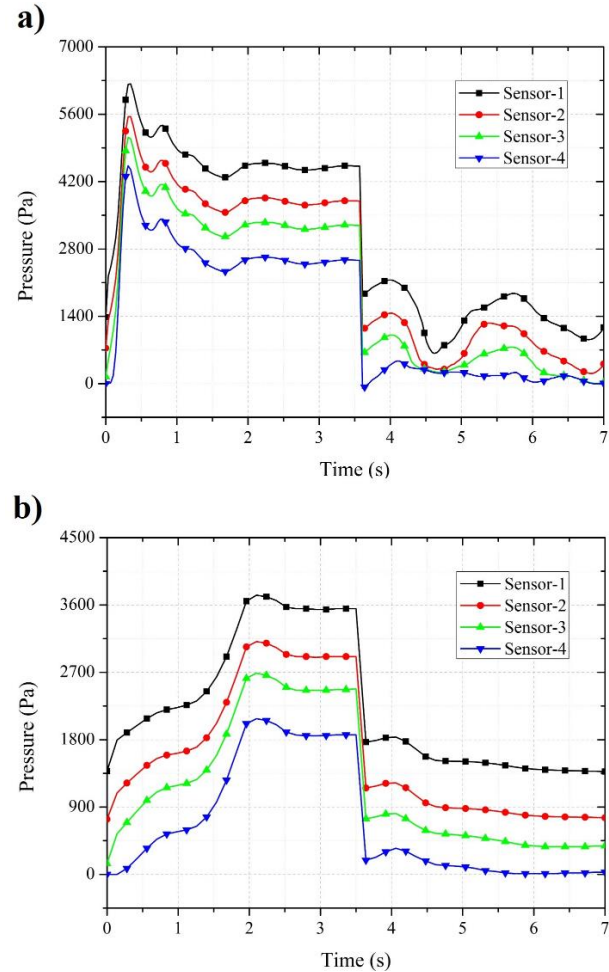


Fig. 5. The pressure history curves of sloshing for a) 60% fill level without baffle and b) 60% fill level with baffle

#### 4. Conclusions

In this study, the fuel tanks of a heavy vehicle with an EBS braking system were analyzed in 6 cases with and without anti-slosh baffles at 25%, 50%, and 60% diesel fuel filling levels. Using anti-slosh baffles reduced the high impact pressures, sudden pressure rises, and large-scale liquid sloshing on the fuel tank walls. This situation positively affects noise and vibration generation, tank damage, and stability disturbances. The anti-slosh baffles prevented high accelerations acting on the tank, pulling fuel from the tank bottom and interrupting the fuel system. This design is also thought to reduce HC formation in gasoline vehicles. In future studies, it is aimed to minimize liquid sloshing, tank weight, and cost by changing the fuel type, fuel tank design, number, location, and geometry of the anti-slosh baffles.

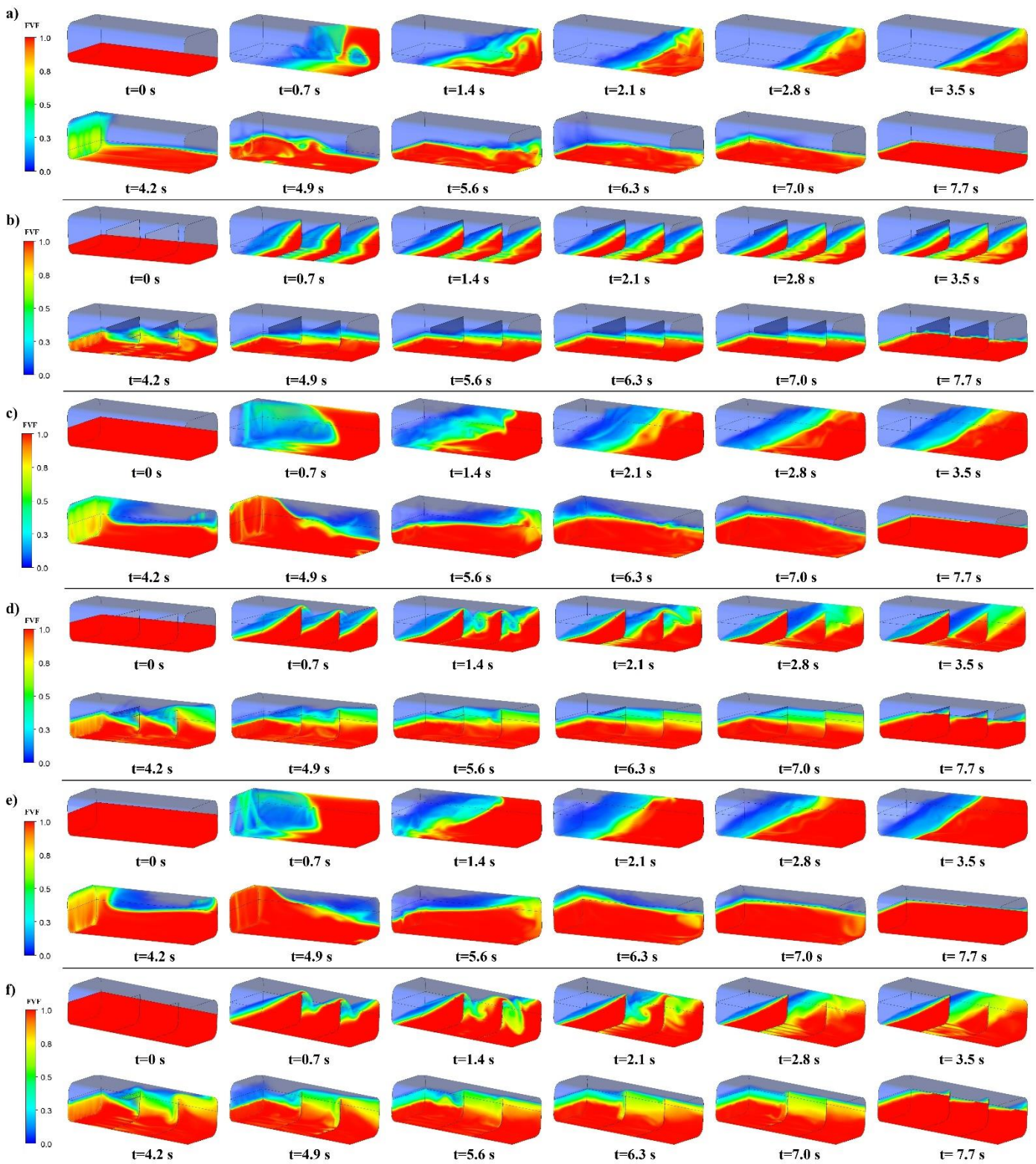


Fig. 6. Fuel volume fraction at various time steps for a) 25% fill level without baffle, b) 25% fill level with baffle, c) 50% fill level without baffle, d) 50% fill level with baffle, e) 60% fill level without baffle, and f) 60% fill level with baffle

## Nomenclature

ALE	: Arbitrary Lagrangian-Eulerian
CFD	: Computational Fluid Dynamics
EBS	: Emergency Braking System
FVF	: Fuel Volume Fraction
HC	: Hydrocarbon
PISO	: Pressure Implicit with Split Operator
RNG	: Renormalization Group
SPH	: Smoothed Particle Hydrodynamics
SST	: Shear Stress Transport
VOF	: Volume of Fluid
$a_b$	: Braking acceleration
$\alpha$	: Volume fraction
$\varepsilon$	: Turbulence dissipation rate
$g$	: Gravitational acceleration
$G_b$	: Turbulent kinetic energies due to the buoyancy
$G_k$	: Turbulent kinetic energies due to the mean velocity gradients
$G_{1\varepsilon}, G_{2\varepsilon}, C_{3\varepsilon}$	: Model constants
$k$	: Turbulent kinetic energy
$\dot{m}_{xy}$	: Mass transfer from phase x to phase y
$\mu$	: Viscosity
$\mu_t$	: Turbulent viscosity
$P$	: Pressure
$\rho$	: Density
$S$	: Stopping distance
$S_x$	: User-defined source for x
$\sigma_x$	: Turbulent Prandtl numbers for x
$t$	: Time
$t_r$	: Reaction time
$t_s$	: Stopping time
$\tau$	: Internal stress forces
$\vec{v}$	: Velocity
$V_0$	: Vehicle speed
$\omega$	: Turbulence dissipation rate
$Y_M$	: Contribution of the fluctuating dilatation in compressible turbulence to the overall dissipation rate
$\nabla$	: Divergence

## Conflict of Interest Statement

The authors declare that there is no conflict of interest in the study.

## CRediT Author Statement

**Turan Alp Arslan:** Software, Methodology, Writing-original draft, Conceptualization, **Hüseyin Bayrakçeken:** Conceptualization, Supervision, **Hicri Yavuz:** Writing-original draft, Visualization

## References

- [1] Zhang E, Zhu W, Wang L. Influencing Analysis of Different Baffle Factors on Oil Liquid Sloshing in Automobile Fuel Tank. Proceedings of the Institution of Mechanical Engineers, Part D: Journal of Automobile Engineering. 2020; 234(13): 3180-3193.
- [2] He R, Zhang E, Fan B. Numerical Analysis on the Sloshing of Free Oil Liquid Surface Under the Variable Conditions of Vehicle. Advances in Mechanical Engineering. 2019; 11(2): 1-13.
- [3] Topçu EE, Kılıç E. A Numerical Investigation of Sloshing in a 3D Prismatic Tank with Various Baffle Types, Filling Rates, Input Amplitudes and Liquid Materials. Applied Sciences. 2023; 13(4): 2474.
- [4] Al-Zughaibi AI, Hussein EQ, Rashid FL. Studying and Analysis of Nonlinear Sloshing (Vibrating) of Interaction Fluid Structure in Storage Tanks. Journal of Mechanical Engineering Research and Developments. 2021; 44(7): 180-191.
- [5] Akyıldız H, Ünal NE. Sloshing in a Three-Dimensional Rectangular Tank: Numerical Simulation and Experimental Validation. Ocean Engineering. 2006; 33(16): 2135-2149.
- [6] Topçu EE, Kılıç E, Çavdar K, Kuzucu İ. Investigation of Sloshing in a Prismatic Tank Filled with Different Liquid Level. The Online Journal of Science and Technology. 2017; 7(4): 115-120.
- [7] Ibrahim RA. Liquid Sloshing Dynamics: Theory and Applications. Cambridge University Press: New York, USA, 2005.
- [8] Akyıldız H, Ünal NE, Aksoy H. An Experimental Investigation of the Effects of the Ring Baffles on Liquid Sloshing in a Rigid Cylindrical Tank. Ocean Engineering. 2013; 59: 190-197.
- [9] Ingle WP, Nalawade D, Jagadale M. Comparative Study of Sloshing Phenomenon in a Tank Using CFD. International Engineering Research Journal. 2017; SE PGCON-MECH-2017: 1-5.
- [10] Mahmud MA, Khan RI, Wang S, Xu Q. Comprehensive Study on Sloshing Impacts for an Offshore 3D Vessel via the Integration of Computational Fluid Dynamics Simulation, Experimental Unit, and Artificial Neural Network Prediction. Industrial & Engineering Chemistry Research. 2020; 59(51): 22187-22204.
- [11] Eswaran M, Saha UK, Maity D. Effect of Baffles on a Partially Filled Cubic Tank: Numerical Simulation and Experimental Validation. Computers & Structures. 2009; 87(3-4): 198-205.
- [12] Rajagounder R, Mohanasundaram GV, Kalakkath P. A Study of Liquid Sloshing in an Automotive Fuel Tank under Uniform Acceleration. Engineering Journal. 2016; 20(1): 71-85.
- [13] Singal V, Bajaj J, Awalgaonkar N, Tibdewal S. CFD Analysis of a Kerosene Fuel Tank to Reduce Liquid Sloshing. Procedia Engineering. 2014; 69: 1365-1371.
- [14] Hasheminejad SM, Mohammadi MM. Effect of Anti-Slosh Baffles on Free Liquid Oscillations in Partially Filled Horizontal Circular Tanks. Ocean Engineering. 2011; 38(1): 49-62.
- [15] Duran S, Coşkun Y, Kılıç D, Uyumaz A, Zengin B. Determination of the Load Applied to Bale Wrapping Machine Rotary Arm and Performing of Design Optimization. Engineering Perspective. 2021; 1(4): 110-114.
- [16] Binboğa F, Şimşek HE. Design and Optimization of a Semi-Trailer Extendable RUPD According to UNECE R58. Engineering Perspective. 2022; 2(2): 13-20.
- [17] Karaman M, Öztürk E. Analysis of the Behavior of a Cross-Type Hydraulic Outrigger and Stabilizer Operating Under Determined

- Loads. *Engineering Perspective*. 2021; 1(1): 22-29.
- [18] Theogene N, Mathieu N, Gebre A. Optimization of Concrete Sleepers Subjected to Static and Impact Loadings. *Engineering Perspective*. 2021; 1(3): 92-98.
- [19] Micheli GB, Fogal MLF, Scalon VL, Padilha A, Ismail KAR. Analysis and Reduction of the Sloshing Phenomena Due to Sudden Movement of Spray Mixture Tanker. *Journal of Applied Fluid Mechanics*. 2022; 15(2): 399-413.
- [20] Scurtu IL, Gheres M, Jurco AN. Sloshing Simulation of the Liquid From the Truck Tanker. *International Symposium, ISB-INMA TEH' 2018, Agricultural and Mechanical Engineering*. Bucharest/Romania, November 2018.
- [21] Arslan TA, Solmaz H, İpci D. Rhombic Mekanizmalı Beta Tipi Bir Stirling Motorunun Adyabatik Şartlarda CFD Analizi. 2nd International Symposium on Automotive Science and Technology. Ankara/Turkey, September 2021.
- [22] Arslan TA, Solmaz H, İpci D, Aksoy F. Investigation of the Effect of Compression Ratio on Performance of a Beta Type Stirling Engine with Rhombic Mechanism by CFD Analysis. *Environmental Progress & Sustainable Energy*. 2023; 42(4): e14076.
- [23] Halis S, Solmaz H, Polat S, Yücesu H. Numerical Study of the Effects of Lambda and Injection Timing on RCCI Combustion Mode. *International Journal of Automotive Science and Technology*. 2022; 6(2): 120-126.
- [24] Nicolici S, Bilegan RM. Fluid Structure Interaction Modeling of Liquid Sloshing Phenomena in Flexible Tanks. *Nuclear Engineering and Design*. 2013; 258: 51-56.
- [25] Calderon-Sanchez J, Gonzalez LM, Marrone S, Colagrossi A, Gambioli F. A SPH Simulation of the Sloshing Phenomenon Inside Fuel Tanks of the Aircraft Wings. 14th International SPHERIC Workshop. Exeter/United Kingdom, June 2019.
- [26] Hirt CW, Nichols BD. Volume of Fluid (VOF) Method for the Dynamics of Free Boundaries. *Journal of Computational Physics*. 1981; 39(1): 201-225.
- [27] Hosain ML, Sand U, Fdhila RB. Numerical Investigation of Liquid Sloshing in Carrier Ship Fuel Tanks. *IFAC-PapersOnLine*. 2018; 51(2): 583-588.
- [28] Rebollo XV, Sadeghi E, Kusano I, Garcia-Granada A-A. Study of the Sloshing Dynamics in Partially Filled Rectangular Tanks with Submerged Baffles Using VOF and LES Turbulence Methods for Different Impact Angles. *Computation*. 2022; 10(12): 225.
- [29] Wei G, Zhang J. Numerical Study of the Filling Process of a Liquid Hydrogen Storage Tank Under Different Sloshing Conditions. *Processes*. 2020; 8(9): 1020.
- [30] Wright MD, Gambioli F, Malan AG. CFD Based Non-Dimensional Characterization of Energy Dissipation Due to Vehicle Slosh. *Applied Sciences*. 2021; 11(21): 10401.
- [31] Sanapala VS, Rajkumar M, Velusamy K, Patnaik BSV. Numerical Simulation of Parametric Liquid Sloshing in a Horizontally Baffled Rectangular Container. *Journal of Fluids and Structures*. 2018; 76: 229-250.
- [32] Siraye W, Wakjira A, Nallamotheu RB. An Analysis of Fuel Oil Sloshing in Partially Filled Cargo Tanker Trucks under Cornering Conditions Using Various Baffle Systems. *Journal of Engineering*. 2023; 9941864.
- [33] Sances D, Gangadharan S, Sudermann J, Marsell B. CFD Fuel Slosh Modeling of Fluid-Structure Interaction in Spacecraft Propellant Tanks with Diaphragms. 51st AIAA/ASME/ASCE/AHS/ASC Structures, Structural Dynamics, and Materials Conference. Florida/USA, April 2010.
- [34] Zhang C. Application of an Improved Semi-Lagrangian Procedure to Fully-Nonlinear Simulation of Sloshing in Non-Wall-Sided Tanks. *Applied Ocean Research*. 2015; 51: 74-92.
- [35] Mahfoze OA, Liu W, Longshaw SM, Skillen A, Emerson DR. On the Efficacy of Turbulence Modelling for Sloshing. *Applied Sciences*. 2022; 12(17): 8851.
- [36] Liu D, Tang W, Wang J, Xue H, Wang K. Comparison of Laminar Model, RANS, LES and VLES for Simulation of Liquid Sloshing. *Applied Ocean Research*. 2016; 59: 638-649.
- [37] Brown SA, Greaves DM, Magar V, Conley DC. Evaluation of Turbulence Closure Models Under Spilling and Plunging Breakers in the Surf Zone. *Coastal Engineering*. 2016; 114: 177-193.
- [38] Tahmasebi MK, Shamsoddini R., Abolpour B. Performances of Different Turbulence Models for Simulating Shallow Water Sloshing in Rectangular Tank. *Journal of Marine Science and Application*. 2020; 19(3): 381-387.
- [39] Ha M, Kim D, Choi HI, Cheong C, Kwon SH. Numerical and Experimental Investigations into Liquid Sloshing in a Rectangular Tank. The 2012 World Congress on Advances in Civil, Environmental, and Materials Research (ACEM' 12). Seoul/ Korea, August 2012
- [40] Kadkhodapour J, Schmauder S, Sajadi F. *Quality Analysis of Additively Manufactured Metals*. Elsevier, 2022.
- [41] Arslan TA. Rhombic Mekanizmalı Beta Tipi Bir Stirling Motorunda Sıkıştırma Oranının Motor Performansına Etkilerinin Sayısal Olarak İncelenmesi. Master Thesis, Gazi University, Ankara, Turkey, 2021.
- [42] Bayrakçeken H, Düzgün M. Vehicles Brake Efficiency and Braking Distance Analysis. *Journal of Polytechnic*. 2005; 8(2): 153-160.
- [43] Latif H, Hultmark G, Rahmana S, Maccarini A, Afshari A. Performance Evaluation of Active Chilled Beam System for Office Buildings - A Literature Review. *Sustainable Energy Technologies and Assessments*. 2022; 52: 101999.
- [44] Ermiş K, Çalışkan M, Okan A. The Effects of Surface Roughness on the Aerodynamic Drag Coefficient of Vehicles. *International Journal of Automotive Science and Technology*. 2022; 6(2): 189-195.
- [45] Seif MS, Asnaghi A, Jahanbakhsh E. Implementation of PISO Algorithm for Simulating Unsteady Cavitating Flows. *Ocean Engineering*. 2010; 37: 1321-1336.